Decoupling of mechanical systems based on in-situ frequency response functions : the link-preserving, decoupling method

Decoupling of mechanical systems based on in-situ frequency response functions: the link-preserving, decoupling method

Laurent Keersmaekers[a,b,*], Luc Mertens[a], Rudi Penne[a,c], Patrick Guillaume[b], Gunther Steenackers[a,b]

[a] *Department of Applied Engineering (FTI),University of Antwerp, Op3Mech, Salesianenlaan 90, B-2660 Hoboken, Belgium*
[b] *Department of Mechanical Engineering (MECH), Vrije Universiteit Brussel, Acoustics & Vibration Research Group (AVRG), Pleinlaan 2, B-1050, Brussels, Belgium*
[c] *Department of Mathematics, University of Antwerp, Middelheimlaan 1, B-2020 Antwerpen, Belgium*

Abstract

Mechanical structures often consist of active and passive parts, the former containing the sources, the latter the transfer paths and the targets. The active and passive parts are connected to each other by means of links. In this article, an innovative theoretical model has been developed to achieve the mathematical decoupling of such structures without disassembling the substructures, when the links connecting the structures are resilient enough. This procedure is required to identify components causing a specific Noise, Vibration and Harsh-ness (NVH) problem. The links are regarded as a parallel connection of springs and dampers, ignoring some physical properties. However, the new procedure will provide a powerful construction in which different link models can be investigated. Therefore, this procedure will be called the *Link-Preserving, Decoupling Method* (LPD method). The absence of a time-consuming physical decoupling procedure distinguishes the LPD method from all known methods such as the classical TPA method. The LPD method is validated by two numerical simulations using linear and nonlinear lumped parameter models and by an experimental case study.

Keywords: LPD, TPA, Decoupling, Lumped parameters, Mechanical vibrations, Modal analysis

*Corresponding author. Tel. +32(0)497 28 09 18
Email address: laurent.keersmaekers@uantwerpen.be (Laurent Keersmaekers)

1. Introduction

In today's automotive applications, the *Noise, Vibration and Harshness* (NVH) characteristics of a vehicle are one of the key factors to make a design successful. Using sophisticated *Computer Aided Design* (CAD) techniques, a vehicle's design process has been significantly shortened and compared to the last decades the overall quality has improved. This tendency also influenced the consumers, being more critical regarding comfort standards, which required more powerful and accurate tools for NVH troubleshooting. In recent years, a lot of research has been performed in this area. The current state-of-the-art procedures can be found in the works of P. Gajdatsy [1, 2], A. Elliott [3], G. Pavić [4] and A.T. Moorhouse [5] in combination with the more classical textbooks by Ewins [6] and Maia & Silva [7]. Among the *Transfer Path Analysis* (TPA) techniques, two fundamentally different categories exist. The first category uses a load-response approach, while the second category is based on output-only measurements. In the remainder of this paper, only load-response-based measurements are considered.

An example of a case where TPA is useful is shown in Figure 1. In this case the upper and lower substructures are considered a source and a receiver respectively. When dealing with NVH problems at receiver locations, one is interested in identifying the responsible forces. Therefore knowledge of the decoupled system's *Frequency Response Functions* (FRFs), starting at the engine mounts' (links) target sides and ending at the different receiver locations, is required. Throughout the paper the structures containing the sources and receivers are called active and passive systems respectively.

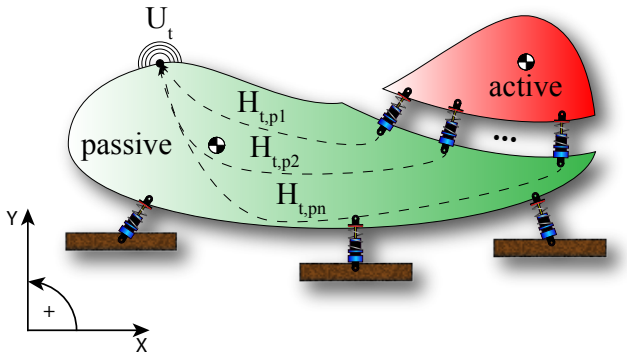

Figure 1: Schematic representation of a TPA case

Theoretically a continuous system containing two substructures, consists of the following set of equations represented in the frequency-domain:

$$\left\{ \begin{array}{c} \mathbf{X}_p(j\omega) \\ \mathbf{X}_a(j\omega) \end{array} \right\} = \left[\begin{array}{cc} \mathbf{H}_{pp}(j\omega) & \mathbf{H}_{pa}(j\omega) \\ \mathbf{H}_{ap}(j\omega) & \mathbf{H}_{aa}(j\omega) \end{array} \right] \left\{ \begin{array}{c} \mathbf{F}_p(j\omega) \\ \mathbf{F}_a(j\omega) \end{array} \right\} \tag{1}$$

The quantities $\mathbf{H}_{ij}$ in Eq. (1) are FRFs with the output and input locations i and j respectively, measured on the coupled system. The subscripts 'p' and 'a' indicate each link's passive and active sides. Figure 2 illustrates the required FRF measurements in the case of the system given by Figure 1. Other quantities are the input force spectra $\mathbf{F}_p$ and $\mathbf{F}_a$ and the output displacement spectra $\mathbf{X}_p$ and $\mathbf{X}_a$.

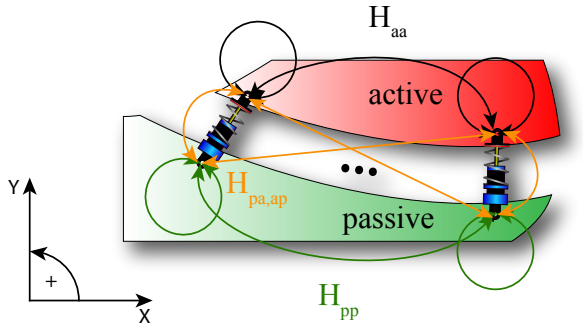

Figure 2: Required FRFs to apply the LPD method

Since the number of Degrees of Freedom (DoFs) for a continuous system is very large, it can easily be observed that only a small part of the entire matrix is measurable . In order to distinguish measurable and immeasurable parts, the former is represented by $\widehat{\bullet}$, the latter by stars. Applying this formulation, Eq. (1) becomes:

$$\begin{Bmatrix} * \\ \widehat{\mathbf{X}}_p(j\omega) \\ \widehat{\mathbf{X}}_a(j\omega) \\ * \end{Bmatrix} = \begin{bmatrix} * & * & * & * \\ * & \widehat{\mathbf{H}}_{pp}(j\omega) & \widehat{\mathbf{H}}_{pa}(j\omega) & * \\ * & \widehat{\mathbf{H}}_{ap}(j\omega) & \widehat{\mathbf{H}}_{aa}(j\omega) & * \\ * & * & * & * \end{bmatrix} \begin{Bmatrix} * \\ \widehat{\mathbf{F}}_p(j\omega) \\ \widehat{\mathbf{F}}_a(j\omega) \\ * \end{Bmatrix} \tag{2}$$

In section 3, theorem 1, it will be shown that the decoupled passive system's FRFs, obtained by the *Link-Preserving, Decoupling* (LPD) method, are expressed as follows:

$$\mathbf{H}_{d,p} = \widehat{\mathbf{H}}_{pp} - \widehat{\mathbf{H}}_{pa}\left(\widehat{\mathbf{H}}_{pa} - \widehat{\mathbf{H}}_{aa}\right)^{-1}\left(\widehat{\mathbf{H}}_{pp} - \widehat{\mathbf{H}}_{ap}\right) \tag{3}$$

where $\mathbf{H}_{d,p}$ is the decoupled passive system's FRF-matrix. These FRFs are illustrated in Figure 3.

It should be noted that by using this formulation the FRFs of the decoupled passive subsystem are obtained without disassembling the system, causing two major advantages. First of all, the entire system remains unchanged providing correct boundary conditions. Secondly, there is no time needed to demount and mount the structure. This advantage distinguishes the LPD method from the existing ones [2], where *a priori* information about the subsystems is always required. This additional information is generally obtained by physically demounting the active subsystem(s). Avoiding this decoupling step leads to a more time-efficient and physically more accurate method. Both advantages will

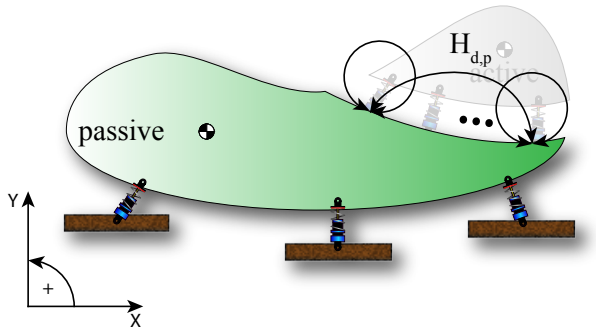

Figure 3: Decoupled system's FRFs

ultimately lead to economical profits due to enhanced customer satisfaction and the benefits of time saving. The advantages and disadvantages are summarised as follows:

advantages:

- *In-situ measurements:* the measurements are performed in-situ, avoiding the decoupling of the active sub-assemblies. This leads to a significant gain in time, which results in financial advantages as well.
- *Correct boundary conditions:* since the active sub-assemblies are coupled to the passive structure at any time, the natural interaction between the passive and active sub-assemblies is maintained. This is important as a structure can only be considered linear in the neighborhood of its working point. Any large deviation such as the removal of a car's engine, leads to erroneous results.
- *Link types:* the LPD method's derivation enables to treat links as parameters. Consequently, different theoretical expressions are obtained. In combination with multibody techniques and the *Finite Element* (FE) method, more advanced links (e.g. containing more DoFs) can be handled.

disadvantages:

- *Force application and sensor placement:* forces must be applied at locations that are sometimes difficult to reach. In some cases the exact locations are not accessible, requiring a point of application in the neighborhood of the desired location. This induces errors in the measured data. Also the placement of sensors is sometimes suboptimal, resulting in (small) deviations compared to real situation.
- *Link types:* not all link types are covered. Depending on the material properties, the geometrical properties and the boundary conditions, longitudinal waves may occur inside the links. This causes difficulties at fre-

quencies above a certain threshold. These situations are not yet covered by the current LPD method.

- *Link rigidity:* the LPD method's current version is limited to cases where the links are considered resilient enough. If links are rigid, it will be impossible to obtain accurate results due to measurement difficulties.

2. Example of a coupled system: a lumped parameter model

The coupling of active and passive subsystems by resilient links is demonstrated using a simple lumped parameter model. Figure 4 shows an example of a 6 Degrees of Freedom (DoF) lumped parameter system. Both the active and the passive subsystem are built with three masses, each of them connected with springs and dampers.

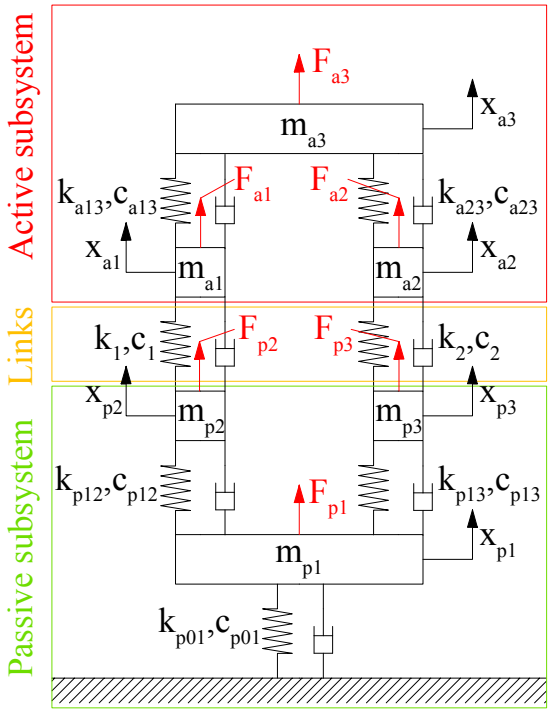

Figure 4: 6 DoF lumped parameter model

This model is the most compact lumped parameter system allowing free motion across each link (denoted by k_1 and k_2), while the passive and active sides are mutually coupled [8]. Every link must be regarded as the parallel connection of a spring and a damper. It is known that a *Multiple Degree of Freedom* (MDoF) system can be described as a linear set of equations. By

assuming the initial conditions to be zero, its Laplace transform results in the following matrix form [9]:

$$\begin{Bmatrix} X_{p1}(s) \\ X_{p2}(s) \\ X_{p3}(s) \\ X_{a1}(s) \\ X_{a2}(s) \\ X_{a3}(s) \end{Bmatrix} = (\mathbf{M}s^2 + \mathbf{C}s + \mathbf{K})^{-1} \begin{Bmatrix} F_{p1}(s) \\ F_{p2}(s) \\ F_{p3}(s) \\ F_{a1}(s) \\ F_{a2}(s) \\ F_{a3}(s) \end{Bmatrix} \tag{4}$$

where $\mathbf{M}$, $\mathbf{C}$ and $\mathbf{K}$ denote the mass, damping and stiffness matrices respectively. X_i and F_i are the Laplace transforms of the displacements x_i and the forces f_i respectively. The mentioned matrices have the following structure:

$$\mathbf{K} = \begin{bmatrix} k_{p01}+k_{p12}+k_{p13} & -k_{p12} & -k_{p13} & 0 & 0 & 0 \\ -k_{p12} & k_{p12}+k_1 & 0 & -k_1 & 0 & 0 \\ -k_{p13} & 0 & k_{p13}+k_2 & 0 & -k_2 & 0 \\ 0 & -k_1 & 0 & k_1+k_{a13} & 0 & -k_{a13} \\ 0 & 0 & -k_2 & 0 & k_2+k_{a23} & -k_{a23} \\ 0 & 0 & 0 & -k_{a13} & -k_{a23} & k_{a13}+k_{a23} \end{bmatrix}$$

$$\mathbf{C} = \begin{bmatrix} c_{p01}+c_{p12}+c_{p13} & -c_{p12} & -c_{p13} & 0 & 0 & 0 \\ -c_{p12} & c_{p12}+c_1 & 0 & -c_1 & 0 & 0 \\ -c_{p13} & 0 & c_{p13}+c_2 & 0 & -c_2 & 0 \\ 0 & -c_1 & 0 & c_1+c_{a13} & 0 & -c_{a13} \\ 0 & 0 & -c_2 & 0 & c_2+c_{a23} & -c_{a23} \\ 0 & 0 & 0 & -c_{a13} & -c_{a23} & c_{a13}+c_{a23} \end{bmatrix}$$

$$\mathbf{M} = \operatorname{diag}\left(\begin{bmatrix} m_{p1} & m_{p2} & m_{p3} & m_{a1} & m_{a2} & m_{a3} \end{bmatrix}\right)$$

where m_i are the masses, c_i the damping coefficients and k_i the spring stiffness's. The corresponding *dynamic stiffness matrix* is defined as [10]:

$$\mathbf{Z}(s) = \mathbf{M}s^2 + \mathbf{C}s + \mathbf{K} \tag{5}$$

Using Eqs. (4) and (5) it is possible to calculate the theoretical FRFs as $\mathbf{H}(s) = \mathbf{Z}^{-1}(s)$. This relation can also be expressed in the frequency-domain by defining $s = j\omega$ [9]. Abbreviating passive parts with a 'p' and active parts with an 'a' the following expression arises:

$$\begin{Bmatrix} X_{p1}(j\omega) \\ X_{p2}(j\omega) \\ X_{p3}(j\omega) \\ X_{a1}(j\omega) \\ X_{a2}(j\omega) \\ X_{a3}(j\omega) \end{Bmatrix} = \begin{bmatrix} H_{p1,p1}(j\omega) & H_{p1,p2}(j\omega) & \cdots & H_{p1,a3}(j\omega) \\ H_{p2,p1}(j\omega) & H_{p2,p2}(j\omega) & \cdots & H_{p2,a3}(j\omega) \\ \vdots & \vdots & \ddots & \vdots \\ H_{a3,p1}(j\omega) & H_{a3,p2}(j\omega) & \cdots & H_{a3,a3}(j\omega) \end{bmatrix} \begin{Bmatrix} F_{p1}(j\omega) \\ F_{p2}(j\omega) \\ F_{p3}(j\omega) \\ F_{a1}(j\omega) \\ F_{a2}(j\omega) \\ F_{a3}(j\omega) \end{Bmatrix} \tag{6}$$

or:

$$\mathbf{X}(j\omega) = \mathbf{H}(j\omega)\mathbf{F}(j\omega) \tag{7}$$

However, as mentioned in section 1, one is interested in the transfer of forces within the passive subsystem. In the case of the presented lumped parameter model, this subsystem can easily be isolated:

$$\begin{Bmatrix} X_{p1}(j\omega) \\ X_{p2}(j\omega) \\ X_{p3}(j\omega) \end{Bmatrix} = (-\mathbf{M}_{d,p}\omega^2 + \mathbf{C}_{d,p}j\omega + \mathbf{K}_{d,p})^{-1} \begin{Bmatrix} F_{p1}(j\omega) \\ F_{p2}(j\omega) \\ F_{p3}(j\omega) \end{Bmatrix} \tag{8}$$

where the subscript 'd' refers to the passive subsystem being decoupled. This expression is equivalent with:

$$\mathbf{X}_{d,p}(j\omega) = \mathbf{H}_{d,p}(j\omega)\mathbf{F}_{d,p}(j\omega) \tag{9}$$

where:

$$\mathbf{K}_{d,p} = \begin{bmatrix} k_{p01}+k_{p12}+k_{p13} & -k_{p12} & -k_{p13} \\ -k_{p12} & k_{p12} & 0 \\ -k_{13} & 0 & k_{p13} \end{bmatrix}$$

$$\mathbf{C}_{d,p} = \begin{bmatrix} c_{p01}+c_{p12}+c_{p13} & -c_{p12} & -c_{p13} \\ -c_{p12} & c_{p12} & 0 \\ -c_{13} & 0 & c_{p13} \end{bmatrix}$$

$$\mathbf{M}_{d,p} = (\begin{bmatrix} m_{p1} & m_{p2} & m_{p3} \end{bmatrix})$$

In real-life conditions, little or even no information is available about $\mathbf{H}_{d,p}(j\omega)$. The ultimate goal of the LPD method is to predict the passive subsystem's FRFs $\mathbf{H}_{d,p}(j\omega)$ by using the coupled system's FRFs $\widehat{\mathbf{H}}(j\omega)$. In the proceeding of this paper, a hat ($\widehat{\bullet}$) will always refer to measured or estimated quantities.

3. The LPD method for parallel connected springs and dampers

Consider a coupled linear(ised) physical system consisting of a passive and an active subsystem, containing N and M DoFs respectively. The system is written as $\mathbf{X} = \mathbf{HF}$, where $\mathbf{X} \in \mathbb{C}^{(N+M)\times 1}$ is the output vector, $\mathbf{F} \in \mathbb{C}^{(N+M)\times 1}$ the input vector and $\mathbf{H} \in \mathbb{C}^{(N+M)\times(N+M)}$ a matrix defining the linearised system.

Theorem 1. *If a system consists of passive and active subsystems, the passive part is constituted as follows:*

$$\boldsymbol{H}_{d,p} = \widehat{\boldsymbol{H}}_{pp} - \widehat{\boldsymbol{H}}_{pa}\left(\widehat{\boldsymbol{H}}_{pa} - \widehat{\boldsymbol{H}}_{aa}\right)^{-1}\left(\widehat{\boldsymbol{H}}_{pp} - \widehat{\boldsymbol{H}}_{ap}\right) \tag{10}$$

where $\mathbf{H}_{d,p}$ is the decoupled passive system's FRF-matrix. $\mathbf{H}_{ij}$ are FRF matrices with the output and input located in the substructures i and j respectively, measured on the coupled system. The subscripts 'a' and 'p' stand for the active and passive subsystems respectively. This situation is illustrated in Figure 2.

Assumption 1. *The system consists of two or more parts, connected by means of links.*

Assumption 2. *The links are considered 'resilient enough' to avoid singularities in Eq. 10.*

Assumption 3. *The links are considered as parallel connections of springs and dampers, allowing translational vibrations only.*

Assumption 4. *The required vibrational information can be measured across each link.*

Proof. The passive and active subsystems are represented in Figure 5. The systems are meshed in order to show that they consist of a large number of DoFs. Each node adds one row and column to the *dynamic stiffness matrix* $\mathbf{Z}$. The mesh size can obviously be reduced, resulting in more nodes. The nodes within the passive subsystem are numbered $1, 2, \ldots, N$, while the nodes within the active subsystem are denoted by $N+1, N+2, \ldots, N+M$. It can easily be noted that N and M represent the number of nodes for the passive and active subsystems respectively.

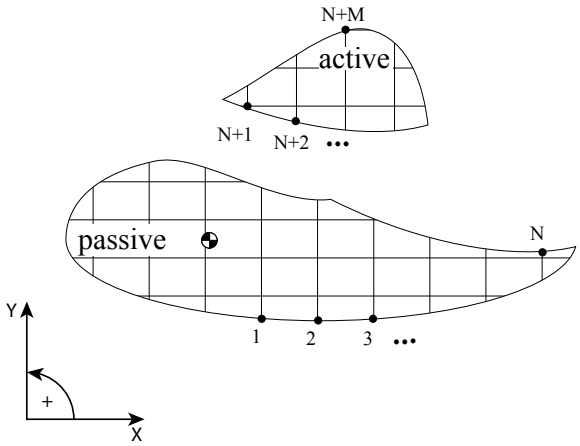

Figure 5: Decoupled passive and active subsystems' mesh

Both subsystems are linked to one another by means of n links, which is illustrated in Figure 6. Each link contains two connection points, linking a passive subsystem's node to the corresponding node within the active subsystem. The passive subsystem's nodes interacting with the links are represented by the last n entries of the numbering sequence:

$$N-n+1, N-n+2, \ldots, N$$

The corresponding nodes within the active system are expressed as:

$$N+1, N+2, \ldots, N+n$$

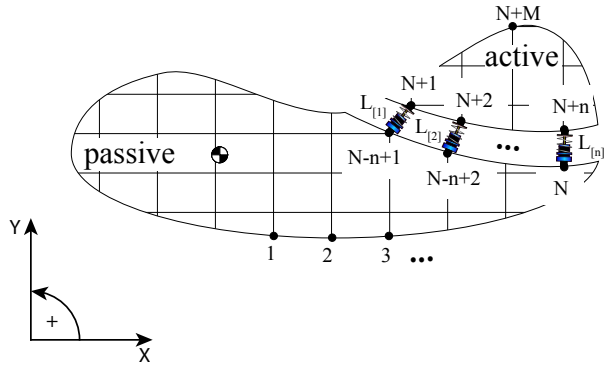

Figure 6: Coupled passive and active subsystems' mesh

Since each link only interacts with its corresponding two nodes within the passive and active subsystems, the link parameters are found in diagonal matrices. From the theory of lumped parameter models and the *Finite Element* (FE) method [10–12], one can verify that linking both subsystems results in the following *dynamic stiffness matrix* $\mathbf{Z}$:

$$\mathbf{Z} = \begin{bmatrix} Z_{1,1} & \cdots & Z_{1,N-n+1} & \cdots & Z_{1,N} & 0 & \cdots & 0 & \cdots & 0 \\ \vdots & \ddots & \vdots & \ddots & \vdots & \vdots & \ddots & \vdots & \ddots & \vdots \\ Z_{N-n+1,1} & \cdots & Z_{N-n+1,N-n+1}+L_1 & \cdots & Z_{N-n+1,N} & -L_1 & \cdots & 0 & \cdots & 0 \\ \vdots & \ddots & \vdots & \ddots & \vdots & \vdots & \ddots & \vdots & \ddots & \vdots \\ Z_{N,1} & \cdots & Z_{N,N-n+1} & \cdots & Z_{N,N}+L_n & 0 & \cdots & -L_n & \cdots & 0 \\ 0 & \cdots & -L_1 & \cdots & 0 & Z_{N+1,N+1}+L_1 & \cdots & Z_{N+1,N+n} & \cdots & Z_{N+1,N+M} \\ \vdots & \ddots & \vdots & \ddots & \vdots & \vdots & \ddots & \vdots & \ddots & \vdots \\ 0 & \cdots & 0 & \cdots & -L_n & Z_{N+n,N+1} & \cdots & Z_{N+n,N+n}+L_n & \cdots & Z_{N+n,N+M} \\ \vdots & \ddots & \vdots & \ddots & \vdots & \vdots & \ddots & \vdots & \ddots & \vdots \\ 0 & \cdots & 0 & \cdots & 0 & Z_{N+M,N+1} & \cdots & Z_{N+M,N+n} & \cdots & Z_{N+M,N+M} \end{bmatrix} \tag{11}$$

In this expression the entire decoupled passive subsystem's *dynamic stiffness matrix* is formed by the matrix entries $Z_{1,1} \ldots Z_{N,N}$:

$$\mathbf{Z}_p = \begin{bmatrix} Z_{1,1} & \cdots & Z_{1,N} \\ \vdots & \ddots & \vdots \\ Z_{N,1} & \cdots & Z_{N,N} \end{bmatrix}$$

Equivalently, the entire active subsystem is denoted as follows:

$$\mathbf{Z}_a = \begin{bmatrix} Z_{N+1,N+1} & \cdots & Z_{N+1,N+M} \\ \vdots & \ddots & \vdots \\ Z_{N+M,N+1} & \cdots & Z_{N+M,N+M} \end{bmatrix}$$

When focussing on the link connection points only, the other matrix elements of the *dynamic stiffness matrix* $\mathbf{Z}$ can be handled as wildcards:

$$\mathbf{Z} = \begin{bmatrix} * & * & \mathbf{0} & \mathbf{0} \\ * & \mathbf{Z}_{d,p}+\mathbf{L}' & -\mathbf{L}' & \mathbf{0} \\ \mathbf{0} & -\mathbf{L}' & \mathbf{Z}_{d,a}+\mathbf{L}' & * \\ \mathbf{0} & \mathbf{0} & * & * \end{bmatrix} \tag{12}$$

where:

$$\mathbf{Z}_{d,p} = \begin{bmatrix} Z_{N-n+1,N-n+1} & \cdots & Z_{N-n+1,N} \\ \vdots & \ddots & \vdots \\ Z_{N,N-n+1} & \cdots & Z_{N,N} \end{bmatrix}$$

and:

$$\mathbf{Z}_{d,a} = \begin{bmatrix} Z_{N+1,N+1} & \cdots & Z_{N+1,N+n} \\ \vdots & \ddots & \vdots \\ Z_{N+n,N+1} & \cdots & Z_{N+n,N+n} \end{bmatrix}$$

Obviously, $\mathbf{Z}_{d,p}$ and $\mathbf{Z}_{d,a}$ are the decoupled subsystems' *dynamic stiffness matrices* defined between the link connection points.

It should be noted that the link parameters $[L_1 \cdots L_n]$ are independent of the active and passive subsystems. In this particular case the link parameters are located on sub-diagonal matrices:

$$\mathbf{L}' = \text{diag}\left(\begin{bmatrix} L_1 & \cdots & L_n \end{bmatrix}\right) \tag{13}$$

From linear algebra, it is obvious that the following expression is valid, taking into consideration that $\mathbf{Z}$ is nonsingular:

$$\mathbf{Z}\mathbf{Z}^{-1} = \mathbf{I} \tag{14}$$

Splitting $\mathbf{Z}$ in a first part containing the systems $\mathbf{Z}_{d,p}$ and $\mathbf{Z}_{d,a}$, and a second part containing the link parameters, results in:

$$\left(\begin{bmatrix} * & * & \mathbf{0} & \mathbf{0} \\ * & \mathbf{Z}_{d,p} & \mathbf{0} & \mathbf{0} \\ \mathbf{0} & \mathbf{0} & \mathbf{Z}_{d,a} & * \\ \mathbf{0} & \mathbf{0} & * & * \end{bmatrix} + \begin{bmatrix} \mathbf{0} & \mathbf{0} & \mathbf{0} & \mathbf{0} \\ \mathbf{0} & \mathbf{L}' & -\mathbf{L}' & \mathbf{0} \\ \mathbf{0} & -\mathbf{L}' & \mathbf{L}' & \mathbf{0} \\ \mathbf{0} & \mathbf{0} & \mathbf{0} & \mathbf{0} \end{bmatrix} \right) \mathbf{H} = \mathbf{I} \tag{15}$$

In this expression $\mathbf{Z}^{-1} = \mathbf{H}$. For presentational reasons a more symbolic expression is introduced:

$$\left(\mathbf{Z}_1 + \begin{bmatrix} \mathbf{0} & \mathbf{0} & \mathbf{0} \\ \mathbf{0} & \mathbf{L} & \mathbf{0} \\ \mathbf{0} & \mathbf{0} & \mathbf{0} \end{bmatrix} \right) \mathbf{H} = \mathbf{I} \tag{16}$$

with:

$$\mathbf{Z}_1 = \begin{bmatrix} * & * & \mathbf{0} & \mathbf{0} \\ * & \mathbf{Z}_{d,p} & \mathbf{0} & \mathbf{0} \\ \mathbf{0} & \mathbf{0} & \mathbf{Z}_{d,a} & * \\ \mathbf{0} & \mathbf{0} & * & * \end{bmatrix}$$

$$\mathbf{L} = \begin{bmatrix} \mathbf{L}' & -\mathbf{L}' \\ -\mathbf{L}' & \mathbf{L}' \end{bmatrix}$$

Pre-multiplying Eq. (16) by $\mathbf{H}_1$ yields:

$$\mathbf{H}_1 \left(\mathbf{Z}_1 + \begin{bmatrix} \mathbf{0} & \mathbf{0} & \mathbf{0} \\ \mathbf{0} & \mathbf{L} & \mathbf{0} \\ \mathbf{0} & \mathbf{0} & \mathbf{0} \end{bmatrix} \right) \mathbf{H} = \mathbf{H}_1 \tag{17}$$

where:

$$\mathbf{H}_1 = \mathbf{Z}_1^{-1}$$

It should be noted that $\mathbf{H}_1$ has the same block structure as $\mathbf{Z}_1$. By using the expression $\mathbf{H}_1\mathbf{Z}_1 = \mathbf{I}$, $\mathbf{H}_1$ can be isolated, resulting in:

$$\mathbf{H}_1 = \mathbf{H}\left(\mathbf{I} - \begin{bmatrix} \mathbf{0} & \mathbf{0} & \mathbf{0} \\ \mathbf{0} & \mathbf{L} & \mathbf{0} \\ \mathbf{0} & \mathbf{0} & \mathbf{0} \end{bmatrix}\mathbf{H}\right)^{-1} \tag{18}$$

Matrix $\mathbf{H}$ consists of a measurable and an immeasurable part. As before the immeasurable part will be denoted by stars, the measurable part by $\widehat{\mathbf{H}}$.

$$\mathbf{H}_1 = \begin{bmatrix} * & * & * \\ * & \widehat{\mathbf{H}} & * \\ * & * & * \end{bmatrix}\left(\mathbf{I} - \begin{bmatrix} \mathbf{0} & \mathbf{0} & \mathbf{0} \\ \mathbf{0} & \mathbf{L} & \mathbf{0} \\ \mathbf{0} & \mathbf{0} & \mathbf{0} \end{bmatrix}\begin{bmatrix} * & * & * \\ * & \widehat{\mathbf{H}} & * \\ * & * & * \end{bmatrix}\right)^{-1} \tag{19}$$

Executing the matrix operations between the brackets leads to:

$$\mathbf{H}_1 = \begin{bmatrix} * & * & * \\ * & \widehat{\mathbf{H}} & * \\ * & * & * \end{bmatrix}\begin{bmatrix} \mathbf{I} & \mathbf{0} & \mathbf{0} \\ * & \mathbf{I}-\mathbf{L}\widehat{\mathbf{H}} & * \\ \mathbf{0} & \mathbf{0} & \mathbf{I} \end{bmatrix}^{-1} \tag{20}$$

Taking into consideration the block structure of $\mathbf{H}_1$, the expression can be written as follows:

$$\begin{bmatrix} * & * & \mathbf{0} & \mathbf{0} \\ * & \mathbf{H}_{d,p} & \mathbf{0} & \mathbf{0} \\ \mathbf{0} & \mathbf{0} & \mathbf{H}_{d,a} & * \\ \mathbf{0} & \mathbf{0} & * & * \end{bmatrix} = \begin{bmatrix} * & * & * \\ * & \widehat{\mathbf{H}} & * \\ * & * & * \end{bmatrix}\begin{bmatrix} \mathbf{I} & \mathbf{0} & \mathbf{0} \\ * & \mathbf{I}-\mathbf{L}\widehat{\mathbf{H}} & * \\ \mathbf{0} & \mathbf{0} & \mathbf{I} \end{bmatrix}^{-1} = \begin{bmatrix} * & * & * \\ * & \widehat{\mathbf{H}} & * \\ * & * & * \end{bmatrix}\begin{bmatrix} \mathbf{I} & \mathbf{0} & \mathbf{0} \\ * & (\mathbf{I}-\mathbf{L}\widehat{\mathbf{H}})^{-1} & * \\ \mathbf{0} & \mathbf{0} & \mathbf{I} \end{bmatrix} \tag{21}$$

It can clearly be observed that the middle section containing $\mathbf{H}_p$ and $\mathbf{H}_a$ results in:

$$\begin{bmatrix} \mathbf{H}_{d,p} & \mathbf{0} \\ \mathbf{0} & \mathbf{H}_{d,a} \end{bmatrix} = \widehat{\mathbf{H}}\left(\mathbf{I} - \mathbf{L}\widehat{\mathbf{H}}\right)^{-1} \tag{22}$$

At this point it can be noted that the system has been mathematically decoupled since the off-diagonal sub-blocks are zero valued matrices. However, the determination of the passive and active subsystems encounters some numerically unstable matrix inversions, resulting in erroneous solutions [13, 14]. Taking into considering the structure of $\mathbf{L}$:

$$\mathbf{L} = \begin{bmatrix} \mathbf{L}' & -\mathbf{L}' \\ -\mathbf{L}' & \mathbf{L}' \end{bmatrix} = \begin{bmatrix} \mathbf{L}' & \mathbf{0} \\ \mathbf{0} & \mathbf{L}' \end{bmatrix}\begin{bmatrix} \mathbf{I} & -\mathbf{I} \\ -\mathbf{I} & \mathbf{I} \end{bmatrix} \tag{23}$$

Eq. (22) is modified as follows:

$$\begin{bmatrix} \mathbf{H}_{d,p} & \mathbf{0} \\ \mathbf{0} & \mathbf{H}_{d,a} \end{bmatrix} = \begin{bmatrix} \widehat{\mathbf{H}}_{pp} & \widehat{\mathbf{H}}_{pa} \\ \widehat{\mathbf{H}}_{ap} & \widehat{\mathbf{H}}_{aa} \end{bmatrix}\left(\begin{bmatrix} \mathbf{I} & \mathbf{0} \\ \mathbf{0} & \mathbf{I} \end{bmatrix} - \begin{bmatrix} \mathbf{L}' & \mathbf{0} \\ \mathbf{0} & \mathbf{L}' \end{bmatrix}\begin{bmatrix} \mathbf{I} & -\mathbf{I} \\ -\mathbf{I} & \mathbf{I} \end{bmatrix}\begin{bmatrix} \widehat{\mathbf{H}}_{pp} & \widehat{\mathbf{H}}_{pa} \\ \widehat{\mathbf{H}}_{ap} & \widehat{\mathbf{H}}_{aa} \end{bmatrix}\right)^{-1} \tag{24}$$

or:

$$\begin{bmatrix} \mathbf{H}_{d,p} & \mathbf{0} \\ \mathbf{0} & \mathbf{H}_{d,a} \end{bmatrix}\left(\begin{bmatrix} \mathbf{I} & \mathbf{0} \\ \mathbf{0} & \mathbf{I} \end{bmatrix} - \begin{bmatrix} \mathbf{L}' & \mathbf{0} \\ \mathbf{0} & \mathbf{L}' \end{bmatrix}\begin{bmatrix} \mathbf{I} & -\mathbf{I} \\ -\mathbf{I} & \mathbf{I} \end{bmatrix}\begin{bmatrix} \widehat{\mathbf{H}}_{pp} & \widehat{\mathbf{H}}_{pa} \\ \widehat{\mathbf{H}}_{ap} & \widehat{\mathbf{H}}_{aa} \end{bmatrix}\right) = \begin{bmatrix} \widehat{\mathbf{H}}_{pp} & \widehat{\mathbf{H}}_{pa} \\ \widehat{\mathbf{H}}_{ap} & \widehat{\mathbf{H}}_{aa} \end{bmatrix} \tag{25}$$

Executing the matrix product between the brackets yields:

$$\begin{bmatrix} \mathbf{H}_{d,p} & \mathbf{0} \\ \mathbf{0} & \mathbf{H}_{d,a} \end{bmatrix} - \begin{bmatrix} \mathbf{H}_{d,p}\mathbf{L}' & \mathbf{0} \\ \mathbf{0} & \mathbf{H}_{d,a}\mathbf{L}' \end{bmatrix}\begin{bmatrix} \widehat{\mathbf{H}}_{pp}-\widehat{\mathbf{H}}_{ap} & \widehat{\mathbf{H}}_{pa}-\widehat{\mathbf{H}}_{aa} \\ \widehat{\mathbf{H}}_{ap}-\widehat{\mathbf{H}}_{pp} & \widehat{\mathbf{H}}_{aa}-\widehat{\mathbf{H}}_{pa} \end{bmatrix} = \begin{bmatrix} \widehat{\mathbf{H}}_{pp} & \widehat{\mathbf{H}}_{pa} \\ \widehat{\mathbf{H}}_{ap} & \widehat{\mathbf{H}}_{aa} \end{bmatrix} \tag{26}$$

The first row of Eq. (26), gives rise to the following expression:

$$\left[\,\mathbf{H}_{d,p}\;\mathbf{0}\,\right] - \mathbf{H}_{d,p}\mathbf{L}'\left[\,\widehat{\mathbf{H}}_{pp}-\widehat{\mathbf{H}}_{ap}\;\widehat{\mathbf{H}}_{pa}-\widehat{\mathbf{H}}_{aa}\,\right] = \left[\,\widehat{\mathbf{H}}_{pp}\;\widehat{\mathbf{H}}_{pa}\,\right] \tag{27}$$

In this expression the left part results in:

$$\mathbf{H}_{d,p} - \mathbf{H}_{d,p}\mathbf{L}'\left(\widehat{\mathbf{H}}_{pp} - \widehat{\mathbf{H}}_{ap}\right) = \widehat{\mathbf{H}}_{pp} \tag{28}$$

or:

$$\mathbf{H}_{d,p} = \widehat{\mathbf{H}}_{pp} + \mathbf{H}_{d,p}\mathbf{L}'\left(\widehat{\mathbf{H}}_{pp} - \widehat{\mathbf{H}}_{ap}\right) \tag{29}$$

The right part of Eq. (27) leads to:

$$-\mathbf{H}_{d,p}\mathbf{L}'\left(\widehat{\mathbf{H}}_{pa} - \widehat{\mathbf{H}}_{aa}\right) = \widehat{\mathbf{H}}_{pa} \tag{30}$$

or:

$$\mathbf{H}_{d,p}\mathbf{L}' = -\widehat{\mathbf{H}}_{pa}\left(\widehat{\mathbf{H}}_{pa} - \widehat{\mathbf{H}}_{aa}\right)^{-1} \tag{31}$$

Merging the expression given by Eq. (31) into Eq. (29) yields:

$$\mathbf{H}_{d,p} = \widehat{\mathbf{H}}_{pp} - \widehat{\mathbf{H}}_{pa}\left(\widehat{\mathbf{H}}_{pa} - \widehat{\mathbf{H}}_{aa}\right)^{-1}\left(\widehat{\mathbf{H}}_{pp} - \widehat{\mathbf{H}}_{ap}\right) \tag{32}$$

This is the final expression for the LPD method when only translational vibrations are considered. Compared to Eq. (22), it can be noted that only one matrix inversion is required since the link parameters are absent. □

It should be noted that the link parameter estimations mathematically disappear, which essentially leads to less matrix inversions. This implies that a higher numerical accuracy is obtained. In theory, the LPD method can be used to decouple any coupled system, as long as the assumptions are met. However, if the links are quasi-rigid it becomes impractical to measure the displacement differences across each link, leading to wrong results. This limits the LPD method to cases where the links are considered resilient enough.

The same derivation can be followed for different link models by adjusting Eq. (12). Obviously, different formulae will be acquired for the estimation of $\mathbf{H}_{d,p}$.

4. The LPD method: numerical case studies

In this section, the theory of the LPD method is applied to two numerical cases. The first case is a 6 DoF lumped parameter model as described in section 2. All components used are assumed to be linear. Using this type of systems, the decoupled model is easily obtained. This allows comparing the theoretical results with the results of the LPD method. Another advantage is the absence of time simulations, which eliminates effects such as leakage and distortions caused by the *Fast Fourier Transform* (FFT). A second case will show the

effects of nonlinearities by using the same lumped parameter system with variant components affected by gravity. Based on the results, it will be argued that the LPD method provides accurate results while the decoupled system leads to erroneous results caused by changed boundary conditions.

4.1. Lumped parameter model: linear system

The model presented first is a 6 DoF lumped parameter model as described in section 2, Figure 4. The theoretical representation of this system is given by Eq. (4):

$$\mathbf{X}(j\omega) = (-\mathbf{M}\omega^2 + \mathbf{C}j\omega + \mathbf{K})^{-1}\mathbf{F}(j\omega)$$

where $\mathbf{M}$, $\mathbf{C}$ and $\mathbf{K}$ are the mass, damping and stiffness matrices, defined in section 2.

In this case one can find an overview of the model parameters in table 4.1. Considering the fact that the system is linear, these parameters are invariant.

System Parameters		
[kg]	[Ns/m]	[N/m]
m_{p1}=30	c_{p01}=500	k_{p01}=6.0×10^6
m_{p2}=40	c_{p12}=550	k_{p12}=5.0×10^6
m_{p3}=30	c_{p13}=500	k_{p13}=3.0×10^6
m_{a1}=20	c_1=550	k_1=4.0×10^6
m_{a2}=30	c_2=500	k_2=6.5×10^6
m_{a3}=50	c_{a13}=550	k_{a13}=2.0×10^6
	c_{a23}=500	k_{a23}=4.0×10^6

Table 1: Model parameters for the linear system

In terms of the FRF-matrix $\mathbf{H}(j\omega)$, Eq. (4) becomes:

$$\mathbf{X}(j\omega) = \mathbf{H}(j\omega)\mathbf{F}(j\omega) \tag{33}$$

where $\mathbf{H}(j\omega)$ is a set of measurable quantities across each link. In this case the measurable part of $\mathbf{H}(j\omega)$ consists of rows 2 to 5 and columns 2 to 5. The new matrix obtained by these entries is denoted by $\widehat{\mathbf{H}}$. Splitting $\widehat{\mathbf{H}}$ in four equally sized parts $\widehat{\mathbf{H}}_{pp}$, $\widehat{\mathbf{H}}_{pa}$, $\widehat{\mathbf{H}}_{ap}$ and $\widehat{\mathbf{H}}_{aa}$ yields:

$$\widehat{\mathbf{H}} = \begin{bmatrix} \widehat{\mathbf{H}}_{pp} & \widehat{\mathbf{H}}_{pa} \\ \widehat{\mathbf{H}}_{ap} & \widehat{\mathbf{H}}_{aa} \end{bmatrix} \tag{34}$$

From Eq. (32) it is known that the expression for the desired passive system is written as follows:

$$(\mathbf{H}_{d,p})_{LPD} = \widehat{\mathbf{H}}_{pp} - \widehat{\mathbf{H}}_{pa}\left(\widehat{\mathbf{H}}_{pa} - \widehat{\mathbf{H}}_{aa}\right)^{-1}\left(\widehat{\mathbf{H}}_{pp} - \widehat{\mathbf{H}}_{ap}\right) \tag{35}$$

Calculating $(\mathbf{H}_{d,p})_{LPD}$ should give the same result as the calculation of the theoretical result:

$$(\mathbf{H}_{d,p})_{th} = (-\mathbf{M}_{d,p}\omega^2 + \mathbf{C}_{d,p}j\omega + \mathbf{K}_{d,p})^{-1} \tag{36}$$

where $\mathbf{M}_{d,p}$, $\mathbf{C}_{d,p}$ and $\mathbf{K}_{d,p}$ are the decoupled passive system's mass, damping and stiffness matrices, defined in section 2.

Illustrating the four possible FRFs between masses m_{p2} and m_{p3} reveals that the results obtained with the LPD method and the theoretical results are identical. This can be observed in Figure 7.

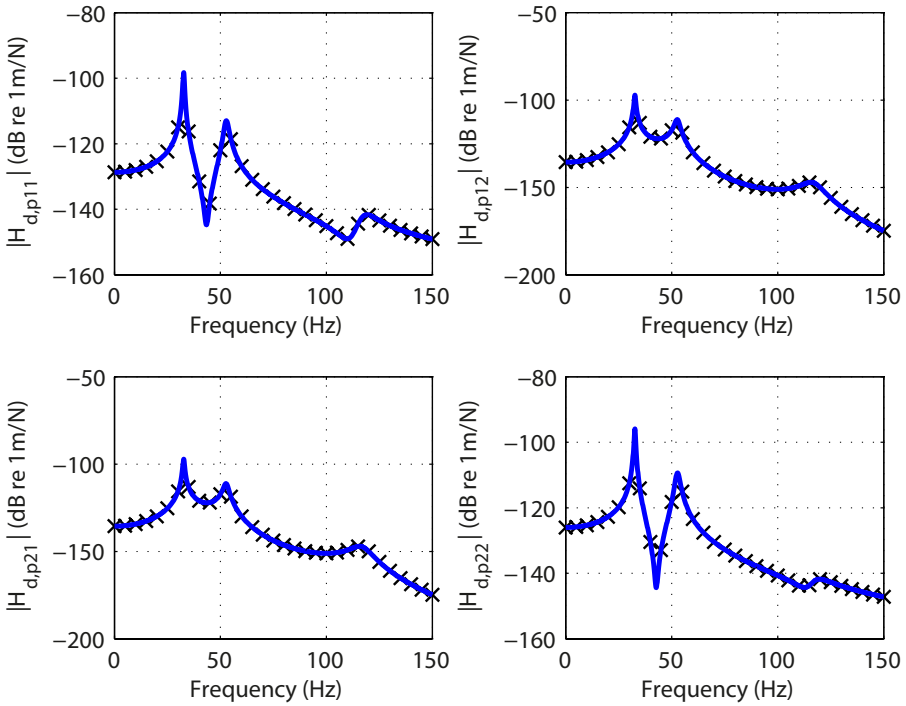

Figure 7: Comparison of FRFs obtained with the LPD method (—) and the theoretical result (X) in the case of a linear system

4.2. Lumped parameter model: nonlinear system

In general the examination of nonlinear systems is only valid in the neighbourhood of the working point. This essentially means that the amplitude variation of acting vibrations is assumed to be relatively small with respect to the local nonlinearity's curvature. In order to prove that decoupling the active system leads to erroneous results in the determination of the passive system's FRFs, the link associated with spring stiffness k_{p01} is made variant with respect to the position x_{p1}. The passive system is therefore represented as shown in Figure 8. For nonlinear systems, determining the accuracy of the method under

investigation (LPD or TPA) is less trivial compared to the linear case, since no reference FRFs are available. Consequently, an alternative reference has to be considered. Another difficulty is encountered when gathering the required FRFs, because a linear analysis such as in section 4.1 may lead to biased results in favour of the LPD method. To handle both issues, time simulations are considered. The resulting time domain vectors are then transformed to the frequency-domain by means of the FFT. In the following paragraphs, it will be explained in detail how the time simulations are performed. To deal with the problem concerning the reference signals, the forces within the links are measured with virtual load sensors ($F_L = k_L\left(x_{La} - x_{Lp}\right) + c_L\left(\dot{x}_{La} - \dot{x}_{Lp}\right)$) and then transformed to the frequency-domain. By using the matrix inversion method [15, 16] on the decoupled system's FRFs obtained by the LPD and TPA methods, similar force spectra should be obtained.

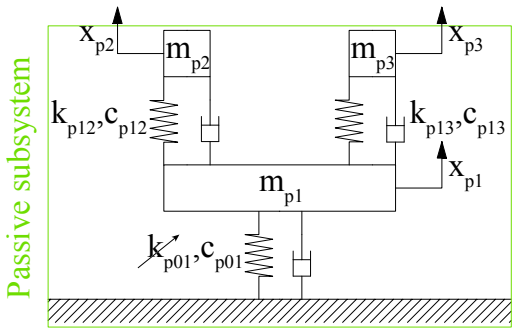

Figure 8: Representation of the passive subsystem with a nonlinear spring k_{p01}

The force exerted on the mass m_{p1} by the nonlinear spring is defined as follows:

$$F_{kp01} = (k_{p01} + \beta x_{p1}^2)x_{p1} \tag{37}$$

where β is a constant that controls the amount of nonlinearity in the spring. The idea to use βx_{p1}^2 originates from Duffing's equation [17]. If β stays within certain limits, '*jumps*' are avoided in the FRFs.

Eq. (37) shows that if the masses m_{a1}, m_{a2} and m_{a3} are removed, $k_{p01}+\beta x_{p1}^2$ will statically be different under the influence of gravity, which essentially leads to a modified working point. In that case the boundary conditions are altered, resulting in different FRF estimates. With the exception of $k_{p01} = 6.0{\times}10^5 N/m$, the same parameters are used as given by table 4.1. The new parameter's value is determined as $\beta = 1.0 \times 10^{14}$.

Input forces

Since time simulations are considered, a proper choice for the input forces must be made. In this case, a pseudo-random force with a constant power spectrum is chosen. The force signal is therefore defined as follows:

$$F(t) = N\text{real}\left[\text{ifft}\left(F_0 \left\{ \begin{smallmatrix} 0 \\ \text{ones}(n,1) \end{smallmatrix} \right\} \circ e^{-2\pi j \text{rand(n+1,1)}}, \text{N}\right)\right] \tag{38}$$

where ifft is the inverse FFT, '$\circ$' the Hadamard or entrywise product, ones $(n, 1)$ a column vector consisting of n elements equal to 1 and rand $(\text{n} + 1, 1)$ a column vector with $n + 1$ uniformly distributed random numbers between 0 and 1. N represents the length of the resulting force vector $F(t)$ and F_0 is the amplitude for each of the harmonic waves within $F(t)$. Note that the DC-component is suppressed to avoid a modified working point. In this section the following constants are chosen:

$$\begin{aligned} N &= 10^4 \\ n &= 150 \\ F_0 &= 0.1 \end{aligned} \tag{39}$$

It can be observed that the period of one force sequence is $1s$ when the sampling frequency f_s equals $10^4 Hz$. In that case, the time vector associated with $F(t)$ is expressed as follows:

$$t = \frac{(0 : N-1)}{f_s} \tag{40}$$

where $(0 : N - 1)$ represents a vector containing all the natural numbers into 0 and $N - 1$ in ascending order.

Setting up the ordinary differential equation solver

An ordinary differential equation (ode) solver is used to calculate the solution of differential equations subjected to initial (and boundary) conditions. Many different ode solvers exist, from which the *Runge-Kutta*4,5 method (ode45) is the most frequently used. In general, the ode45 solver requires three input arguments. The first input argument is a function handle pointing to a file which contains the physics of the investigated problem. The second argument is a vector specifying the interval of integration. To obtain solutions at specific time steps, the argument must be a vector (t in this case). The third argument is a vector containing the initial conditions of the system. In this simulation, the initial displacements and velocities are zero.

Since the ode45 solver can only handle sets of first order differential equations, the N second order equations given by:

$$\mathbf{M}\ddot{\mathbf{x}}(t) + \mathbf{C}\dot{\mathbf{x}}(t) + \mathbf{K}\mathbf{x}(t) = \mathbf{f}(t) \tag{41}$$

must be converted into $2N$ first order equations. This can be achieved by adding the following expression:

$$\mathbf{M}\dot{\mathbf{x}}(t) - \mathbf{M}\dot{\mathbf{x}}(t) = \mathbf{0} \tag{42}$$

In one matrix expression, this becomes:

$$\begin{bmatrix} \mathbf{C} & \mathbf{M} \\ \mathbf{M} & \mathbf{0} \end{bmatrix} \begin{Bmatrix} \dot{\mathbf{x}}(t) \\ \ddot{\mathbf{x}}(t) \end{Bmatrix} + \begin{bmatrix} \mathbf{K} & \mathbf{0} \\ \mathbf{0} & -\mathbf{M} \end{bmatrix} \begin{Bmatrix} \mathbf{x}(t) \\ \dot{\mathbf{x}}(t) \end{Bmatrix} = \begin{Bmatrix} \mathbf{f}(t) \\ \mathbf{0} \end{Bmatrix} \tag{43}$$

or:

$$\mathbf{A}\dot{\mathbf{q}}(t) + \mathbf{B}\mathbf{q}(t) = \mathbf{f}^*(t) \tag{44}$$

with:

$$\mathbf{A} = \begin{bmatrix} \mathbf{C} & \mathbf{M} \\ \mathbf{M} & \mathbf{0} \end{bmatrix}, \qquad \mathbf{B} = \begin{bmatrix} \mathbf{K} & \mathbf{0} \\ \mathbf{0} & -\mathbf{M} \end{bmatrix}, \qquad \mathbf{q}(t) = \begin{Bmatrix} \mathbf{x}(t) \\ \dot{\mathbf{x}}(t) \end{Bmatrix}, \qquad \mathbf{f}^*(t) = \begin{Bmatrix} \mathbf{f}(t) \\ \mathbf{0} \end{Bmatrix}$$

In this expression, $\mathbf{q}(t)$ is the state-vector and $\mathbf{f}^*(t)$ the modified force vector, containing the input forces $F(t)$ and the gravitational force applied on m_i, $i = 1, 2, \ldots, 6$. During each time step, the next state of the system is calculated by solving:

$$\begin{aligned} \dot{\mathbf{q}}_i(t) &= \mathbf{A}_i^{-1} \left(-\mathbf{B}_i \mathbf{q}_i(t) + \mathbf{f}_i^*(t) \right) \\ \mathbf{q}_{i+1}(t) &= f\left(h, \dot{\mathbf{q}}_i(t), \mathbf{q}_i(t) \right) \end{aligned} \tag{45}$$

where h is the time step length used by the solver. This step size varies depending on the desired relative and absolute accuracies, defined by the user.

Simulations

A first simulation is performed on the coupled system to acquire the FRFs for the LPD method. A second simulation is run on the decoupled system in order to apply the TPA method. Both simulations are executed during $10s$ to minimise the transient effects due to the gravitational forces and the external forces' initial application. Since the input force is periodical ($T = 1s$), the last period of $1s$ is used for the further analysis. In the case of the first simulation, the resulting time vectors are transformed to the frequency-domain by means of the FFT to construct the sub-matrices $\widehat{\mathbf{H}}_{pp}$, $\widehat{\mathbf{H}}_{pa}$, $\widehat{\mathbf{H}}_{ap}$ and $\widehat{\mathbf{H}}_{aa}$. The decoupled system is then found by applying the LPD method, resulting in $(\mathbf{H}_{d,p})_{LPD}$. The second simulation's output vectors are directly used to obtain $(\mathbf{H}_{d,p})_{TPA}$. The results of both methods are shown in Figure 9. It can be observed that the influence of one nonlinear element causes different FRFs for the coupled and decoupled systems.

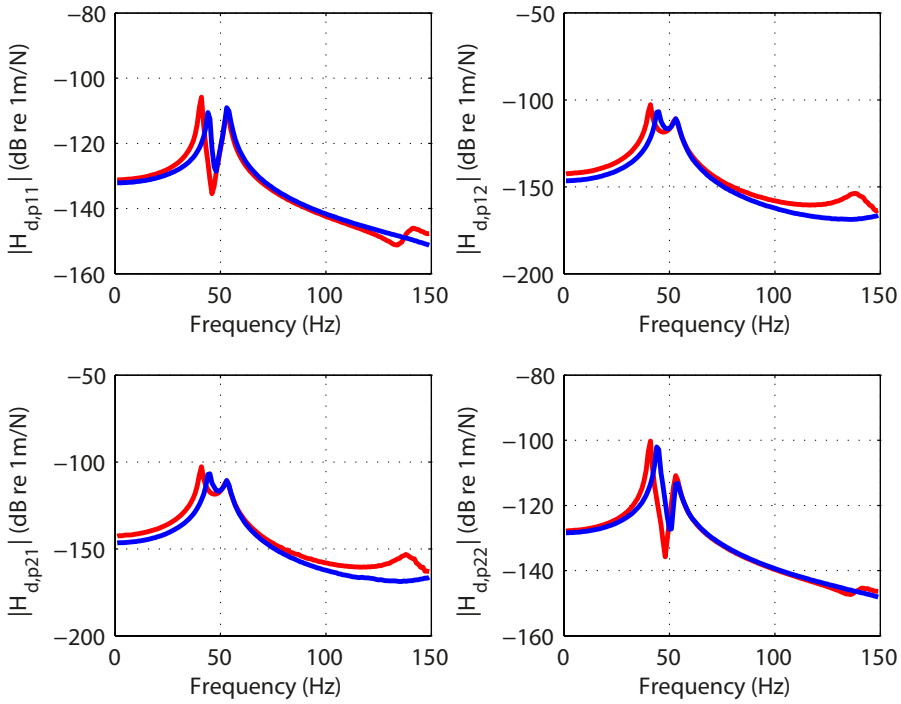

Figure 9: Comparison of the LPD method (—) with the TPA method (—) in the case of a system containing a nonlinear spring

Since there are no reference FRFs available, it is impossible to tell whether the LPD or the TPA method provides the desired results. However, since the link forces are measured as well, the inverse matrix method can be applied to obtain an estimate for these forces. In this case, the link forces are examined when a force is applied at the passive side of link 1:

$$\begin{aligned}(\mathbf{F}_L)^{p1}_{LPD} &= (\mathbf{H}_{d,p})^{-1}_{LPD}\,\mathbf{X}^{p1}_p - \left\{ \begin{smallmatrix} F_{p1} \\ 0 \end{smallmatrix} \right\} \\ (\mathbf{F}_L)^{p1}_{TPA} &= (\mathbf{H}_{d,p})^{-1}_{TPA}\,\mathbf{X}^{p1}_p - \left\{ \begin{smallmatrix} F_{p1} \\ 0 \end{smallmatrix} \right\}\end{aligned} \tag{46}$$

The notations used in this equation follow the descriptions:

- $(\mathbf{F}_L)^{p1}_{LPD}$: the forces exerted by the links applied to the passive subsystem due to the compression and tension. The motions are caused by an external force acting on the passive side of link 1, indicated by the superscript $p1$.
- $\mathbf{X}^{p1}_p$: the displacements measured at the links' passive sides, caused by an external force acting on the passive side of link 1.
- $-\left\{ \begin{smallmatrix} F_{p1} \\ 0 \end{smallmatrix} \right\}$: vector containing the external force acting at the passive side of link 1.

If a force is applied at the the passive side of link 2, one obtains:

$$\begin{aligned}(\mathbf{F}_L)^{p2}_{LPD} &= (\mathbf{H}_{d,p})^{-1}_{LPD}\,\mathbf{X}^{p2}_p - \left\{\begin{smallmatrix}0\\F_{p2}\end{smallmatrix}\right\} \\ (\mathbf{F}_L)^{p2}_{TPA} &= (\mathbf{H}_{d,p})^{-1}_{TPA}\,\mathbf{X}^{p2}_p - \left\{\begin{smallmatrix}0\\F_{p2}\end{smallmatrix}\right\}\end{aligned} \tag{47}$$

The results of both methods and the measured force spectrum are shown in Figure 9. It can be observed that the force spectrum obtained by the LPD method coincides with the expected force spectrum, while the TPA method shows a clear offset. It can therefore be stated that the LPD method is more suited to deal with nonlinear systems compared to the TPA method.

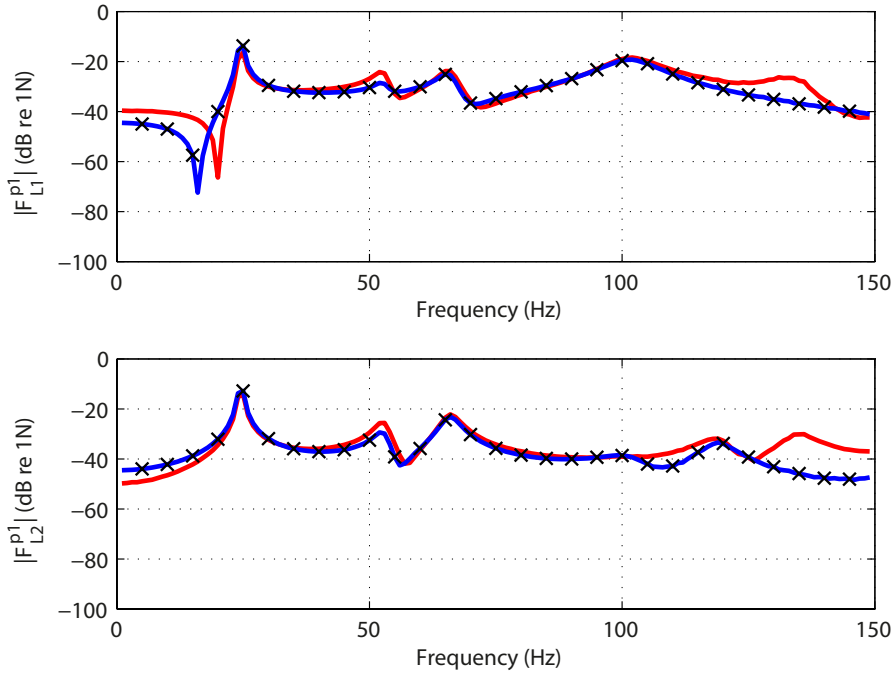

Figure 10: Comparison of the directly measured link forces (X) with the LPD method (—) and the TPA method (—) in the case of a system containing a nonlinear spring

5. The LPD method: experimental case study

In this section, the LPD method is applied to an experimental setup as illustrated in Figure 11. The setup consists of an active (red) and a passive (green) subsystem. The passive subsystem is connected to the environment by means of springs in combination with foam to add damping to the structure. The active and passive subsystems are separated by three springs (links). The accelerations across each link are measured by accelerometers, while the input forces are provided by an impact hammer. The obtained time signals are then

transformed to the frequency-domain using the FFT. The corresponding FRFs are estimated with the H_1 estimator. In this case 10 measurement records are considered per FRF. Each record is captured with a sampling frequency of $5000Hz$ and a length of $10s$.

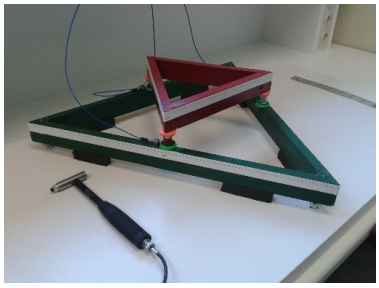

Figure 11: Experimental test setup consisting of an active and a passive subsystem

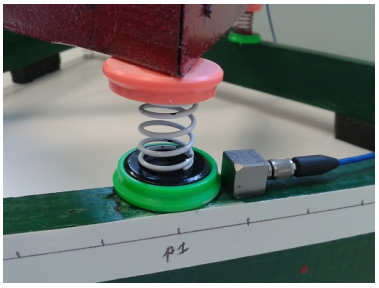

Figure 12: The links separating both subsystems are attached by using magnets

To validate the LPD method, measurements are performed on the decoupled system (TPA method). In Figure 12 it can be observed that switching from the coupled to the decoupled system is an easy task, since the links are connected by magnets. The results obtained after using both the LPD method and the TPA method are illustrated in Figure 13.

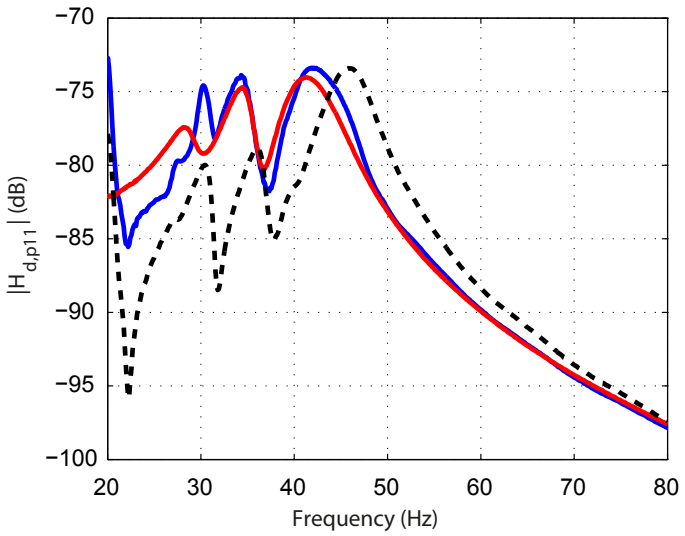

Figure 13: Comparison of the coupled system's FRFs (- -) with the decoupled system's FRFs provided by the LPD method (—) and the TPA method (—) in the case of an experimental setup

It can be observed that the results obtained by the LPD method are similar to those obtained by the TPA method. The observed differences are caused by the misalignment of the applied forces and sensors. Theoretically, one should measure the differential displacements at each spring's centerline, which is impossible since the points of interest are located inside the link. The problem may be solved by measuring more channels per link and averaging the obtained FRFs. However, adding more input/output channels per link causes the number of measurements to increase quadratically. Furthermore, this technique is not valid for the higher frequency range. On the other hand the results obtained by the classical TPA method are not always reliable references, since nonlinearities within the different subsystems may influence the decoupled system's FRFs. Even with those considerations in mind, the relative error between the LPD and the TPA method hardly exceeds $3dB$ in the case of this experiment. This can be observed in Figure 14.

In future research, the effects of sensor/force misalignments will be investigated further.

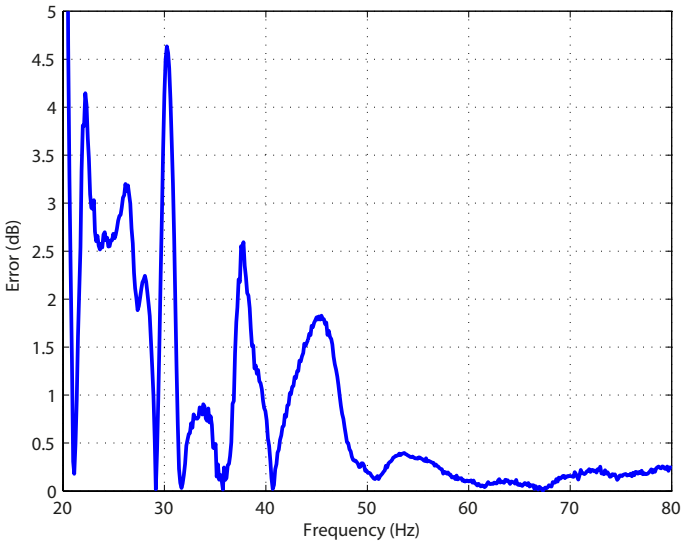

Figure 14: Relative error between the LPD and the TPA method

6. Conclusions

In this article, an innovative theoretical model has been developed to achieve the mathematical decoupling of mechanical structures when the links connecting the structures are resilient enough, without disassembling the substructures. The absence of a time-consuming physical decoupling procedure distinguishes the LPD method from all known methods such as the classical TPA method. The decoupling procedure is required to obtain the passive system's FRFs for

the estimation of the operational forces and path contributions. To validate the theoretical assumptions simulations as well as experiments have been performed. By assuming all components to be linear, the physically decoupled system's FRFs (TPA method) are used as a reference to compare the FRFs obtained by the LPD method. After comparing both methods, one can conclude that the LPD method provides accurate results. Even when both the active and passive subsystems are slightly nonlinear, the LPD method still provides accurate FRF estimates. To demonstrate the method in practice, an experimental case study is considered. The LPD method is applied and the results are compared with the classical TPA method, which served as a benchmark.

Acknowledgements

This research has been funded by the University of Antwerp (FTI-OZC). The authors also acknowledge the research councils of the Vrije Universiteit Brussel (OZR).

References

[1] P. Gajdatsy, et. al. A novel tpa method using parametric load models: validation on experimental and industrial cases. Technical report, SAE Technical Paper, 2009.

[2] P. Gajdatsy. Advanced transfer path analysis methods. PhD thesis, KULeuven, 2009.

[3] G. Pavić, A. Elliott. Structure-borne sound characterization of coupled structures - part i: simple demonstrator model. Journal of Vibration and Acoustics, 132, 2010.

[4] G. Pavić, A. Elliott. Characterisation of structure borne noise in situ. In Proceedings Euronoise, 2006.

[5] A. T. Moorhouse, et. al. In situ measurements of the blocked force of structure-borne sound sources. Journal of sound and vibration, 325(4):679–685, 2009.

[6] D. J. Ewins. Modal testing: theory, practice and application (mechanical engineering research studies: engineering dynamics series). Research studies Pre, 2000.

[7] N. M. M. Maia, J. M. M. Silva. Theoretical and experimental modal analysis. Research Studies Press Taunton, 1997.

[8] G. De Sitter, et. al. Operational transfer path analysis. Mechanical Systems and Signal Processing, 24(2):416–431, 2010.

[9] W. Heylen, P. Sas. Modal analysis theory and testing. Katholieke Universteit Leuven, Departement Werktuigkunde, 2006.

[10] Z. Fu, J. He. Modal analysis. Butterworth-Heinemann, 2001.

[11] O. C. Zienkiewicz, R. L. Taylor. The finite element method: The basis, volume 1. Butterworth-Heinemann, 2000.

[12] O. C. Zienkiewicz, R. L. Taylor. The finite element method: Solid mechanics, volume 2. Butterworth-Heinemann, 2000.

[13] G. H. Golub, C. F. Van Loan. Matrix computations, volume 3. JHU Press, 2012.

[14] H.W. Engl, M. Hanke, A. Neubauer. Regularization of inverse problems, volume 375. Springer, 1996.

[15] J. Plunt. Finding and fixing vehicle nvh problems with transfer path analysis. Sound and vibration, 39(11):12–17, 2005.

[16] The qualification and quantification of vibro-acoustic transfer paths. Technical report, LMS International, 2009.

[17] R. H. Enns. Nonlinear physics with mathematica for scientists and engineers. Birkhuser, 2001.